nol., **13,** 117 (1976).
13. T. Ratcheva and M. Nanova, *Thin Solid Films,* **141,** L87 (1986).
14. M. Inoue, T. Matsuoka, Y. Fujita, and A. Abe, *Jpn. J. Appl. Phys.*, **28,** 274 (1989).
15. W. Huber, *Titrations in Nonaqueous Solvents,* Academic Press, Inc., New York (1967).
16. G. Koch, *Ber. Bunsenges.*, **69,** 141 (1965).
17. D. A. Vermilyea, *This Journal,* **113,** 1067 (1966).
18. N. Valverde, *Ber. Bunsenges.*, **80,** 333 (1976).
19. K. Sangwal, *J. Mater. Sci.*, **15,** 237 (1980).
20. J. J. Ponjeé and H. J. Feil, U.S. Pat. 4,093,504 (1978).
21. N. Valverde, *Ber. Bunsenges. Phys. Chem.*, **92,** 1072 (1988).
22. H. J. Engell, *Z. Phys. Chem. NF.*, **7,** 158 (1956).
23. D. Yohe, A. Riga, R. Greef, and E. Yeager, *Electrochim. Acta,* **13,** 1351 (1968).
24. N. R. Armstrong, A. W. C. Lin, M. Fujihira, and T. Kuwana, *Anal. Chem.*, **48,** 741 (1976).
25. O. M. R. Chyan and K. Rajeshwar, *This Journal,* **132,** 2109 (1985).
26. P. H. L. Notten, *ibid.*, **131,** 2641 (1984).
27. P. H. L. Notten and A. A. J. M. Damen, *Appl. Surf. Sci.*, **28,** 331 (1987).
28. R. M. Smith and A. E. Martel, *Critical Stability Constants,* Vol. 3 and 4, Plenum Press, New York (1976).
29. *Handbook of Chemistry and Physics,* 48th ed., The Chemical Rubber Co., Cleveland, OH (1967-1968).

LPCVD WSi_2 Films Using Tungsten Chlorides and Silane

N. Thomas, P. Suryanarayana,[a] E. Blanquet, C. Vahlas, R. Madar,*[,b] and C. Bernard

LTPCM-ENSEEG, BP 75, 38402 Saint Martin d'Hères, France
[a]SDA, CEERI, Pilani, 333031 India
[b]LMGP-ENSPG, BP 46, 38402 Saint Martin d'Hères, France

ABSTRACT

This paper makes a systematic study of blanket and selective low pressure chemical vapor deposition (LPCVD) WSi_2 films from tungsten chlorides, silane, hydrogen, and argon on silicon as well as on patterned oxidized silicon substrates. Experiments were performed by varying the initial gaseous WCl_4 to SiH_4 ratio (Rx) or the deposition temperature (T_d). Initially, yield and CVD-phase diagrams of the W-Si-Cl-H-Ar chemical system were drawn, based on thermodynamic simulations. The deposition of pure WSi_2 phase and mixed solid phases involving W, W_5Si_3, WSi_2, and Si was predicted to occur in relation to process parameters. The corresponding films were grown in a cold-wall reactor and characterized by x-ray diffraction, scanning electron microscopy, four-point probe, and Auger electron spectroscopy studies. Good agreement was found between experimentally observed solid phases and thermodynamically simulated results, under the same conditions. The growth rate of films for an Rx value varying between 0.3 and 1.0 at 873 K reaches a maximum at $Rx = 0.5$. The Arrhenius plot of films grown between 773 and 1073 K shows a linear increase in growth rate up to 923 K, followed by saturation at high temperatures. Films processed above 823 K have a smooth surface and interface, indicating that the chloride-based chemistry does not affect the silicon substrate even at high temperatures. Based on the above mentioned studies, a set of process parameters was defined, and selective LPCVD WSi_2 films were deposited on fine-patterned oxidized silicon.

The need for a lower resistance material than polysilicon has resulted in the investigation of silicides and refractory metals for very large scale integrated (VLSI) manufacturing. Refractory metals have low bulk resistance, but their poor oxidation characteristics and poor adhesion after annealing have limited their acceptability. Although silicides have higher bulk resistivities than refractory metals, they have advantageous properties such as stability over the range of integrated circuit (IC) wafer processing temperatures, good adhesion, chemical resistance, and dry etchability.[1,2] Refractory metal silicide films can be prepared either by annealing a metal film on Si or a codeposited mixture of metal and silicon on a doped polysilicon layer, or by chemical vapor deposition (CVD).[3,4] Deposition of silicide is preferred to silicide formation by annealing a metal deposit on Si since the latter generally results in a rough silicide/Si interface. For processing of silicide films for micron and submicron devices, chemical vapor deposition techniques have many advantages over physical vapor deposition (PVD), particularly with respect to step coverage, radiation damage, wafer throughput, and control of stoichiometry of the films.[7,8] In addition, CVD presents the possibility of selective deposition, depending on the nature of the substrate, which is a considerable advantage for the preparation of metal silicides for the new generation of ultralarge scale integration (ULSI) devices. The salicide process for contacts, which has an inherent problem of consumption of silicon under metal, may be replaced by selective CVD of metal silicide for shallow junction devices.[9] Selective deposition of $TaSi_2$, and $TiSi_2$ has been reported without consumption of the underlying silicon.[10-12]

WSi_2 films have already been processed using tungsten hexafluoride, WF_6, and SiH_4.[13,14] Although the fluoride-based process has many attractive features, the highly reactive fluoride by-product species present in the gaseous phase attack the substrate and this leads to a textured interface.[15,16] In addition, it has been shown that the formation of pure WSi_2 films is thermodynamically possible only in a very narrow reactant gas-phase composition range.[17-19] A small change in WF_6 or SiH_4 partial pressures can lead to the formation of W_5Si_3-WSi_2 or WSi_2-Si mixtures, so that, under normal operating conditions the formation of pure tungsten disilicide films would be difficult to control. The substitution of tungsten chlorides for tungsten fluorides allows better control over WSi_2 film stoichiometry.[17]

Contrary to other refractory metal chlorides like titanium tetrachloride ($TiCl_4$), which are relatively easy to transport since they are liquid at room temperature, the major concern for the tungsten-chloride-based CVD process is the gas source. The metal chloride vapor can be generated either by evaporation of solid tungsten hexachloride (WCl_6) or by *in situ* chlorination of the metal. Consequently, little work has been reported on the processing of WSi_2 films using chloride-based chemistry in comparison to the fluoride-based chemistry.

Harsta *et al.* processed selective W films using WCl_6 as tungsten source. It was reported that problems of stability of the metal source, etc., lead to poorly reproducible vapor flow.[20] In addition, the corresponding gas line must be heated to avoid condensation of the metal chloride gases in the line. As a result, a CVD system containing an *in situ* chlorination chamber was designed and manufactured. It has been successfully used for the preparation of atmospheric pressure CVD (APCVD) $TaSi_2$,[21] and WSi_2.[22] In a combined thermodynamic and mass spectrometric study of

---

* Electrochemical Society Active Member.

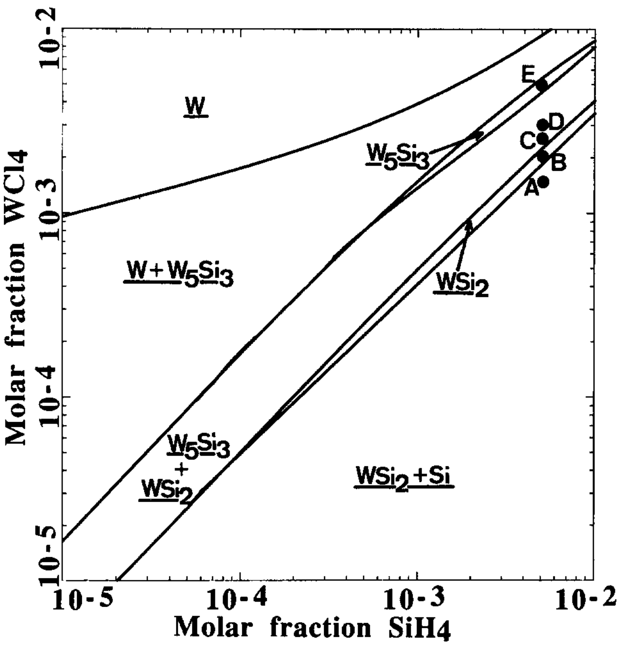

Fig. 1. Thermodynamic simulated W-Si CVD-phase diagram at 1 Torr total pressure and 873 K deposition temperature, $P_{Ar} = 0.9\ P_{tot}$.

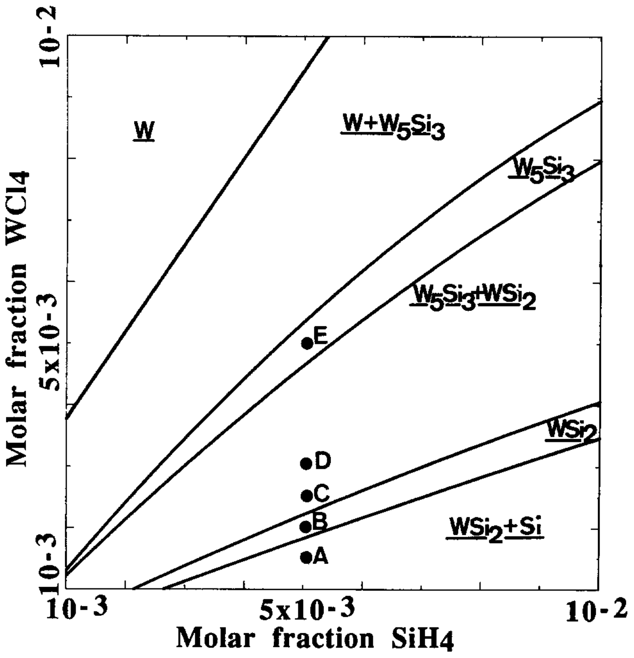

Fig. 2. Magnification of top right region of Fig. 1.

the *in situ* chlorination of tungsten,[23] it was shown that: (*i*) WCl_4 is the major gaseous product of the chlorination process; (*ii*) operating at low pressure facilitates the quantitative production of gaseous chlorides; and (*iii*) there is no free chlorine in the resulting gas phase when the chlorination temperature is higher than 1025 K.

In this paper, a combined thermodynamic and experimental study of blanket and selective LPCVD WSi_2 films is presented, based on the principles of thermochemical modeling of a CVD process.[24] Initially, a thermodynamic simulation of the W-Si-Cl-H-Ar chemical system was made. The results were illustrated by yield and CVD-phase diagrams drawn as a function of reactant ratio or deposition temperature. Based on this theoretical study, two sets of films were prepared: (*i*) blanket LPCVD tungsten silicide films by varying either the initial gaseous WCl_4 to SiH_4 ratio (*Rx*) or the deposition temperature (*Td*), and (*ii*) selective LPCVD pure WSi_2 films on patterned oxidized silicon wafers. These films were characterized by scanning electron microscopy (SEM), x-ray diffraction (XRD), Auger electron microscopy (AES), and four-point probe measurements.

Thermodynamic Simulations

For a given chemical system, a thermodynamic simulation of a CVD process may provide valuable information on the composition of the resulting gaseous and condensed phases at equilibrium as a function of the process parameters.[25]

In the present study, the investigation of LPCVD WSi_2 films was supported by a thermodynamic simulation based on minimization of the Gibbs free energy of the W-Si-Cl-H-Ar chemical system. The thermodynamic data on the species generated in this system were taken from the Scientific Group Thermodata Europe (SGTE) bank. For the species not covered by this data bank, the data were critically selected from the available literature. In particular, data on the two tungsten silicide solid phases: W_5Si_3 and WSi_2 were taken from the work of Vahlas *et al.*[26] where the W-Si binary-phase diagram was calculated on the basis of available thermodynamic and metallurgical informations.

Calculations were made with the MELANGE software.[27] The resulting composition and quantity of deposited solid phases and by-product gas species at equilibrium were represented by CVD-phase and yield diagrams, respectively. The CVD-phase diagrams were first used by Ducarroir[28] to illustrate the thermodynamic simulation of CVD processes. They predict the possible deposition of solid phases as a function of two experimental parameters (here the initial partial pressures of the tungsten and silicon precursors, WCl_4 and SiH_4), for fixed values of the other process

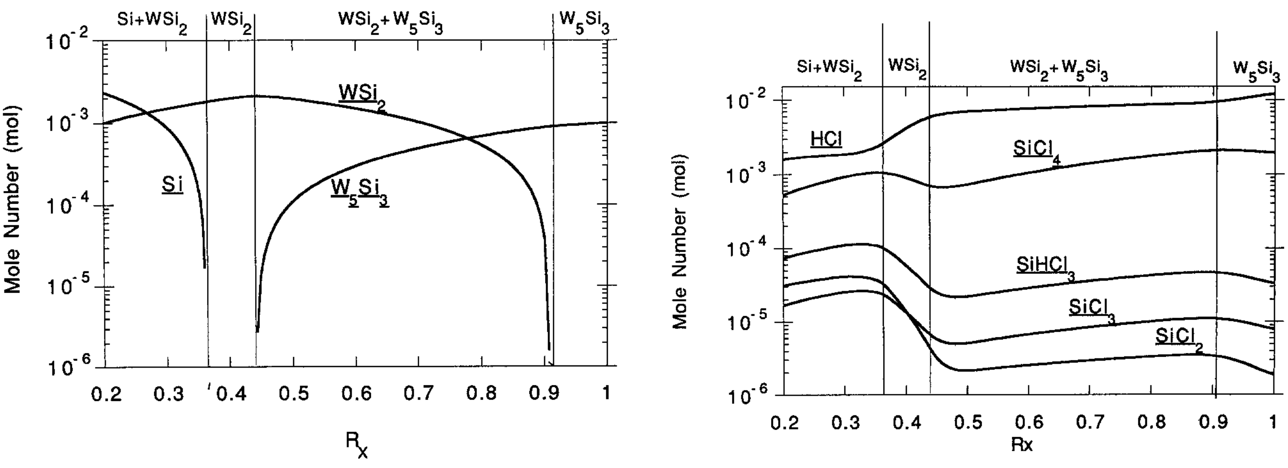

Fig. 3. (a, left) Yield diagram of computed solid phases as a function of reactant ratio (P_{tot} = 1 Torr; T_d = 873 K; $P_{Ar} = 0.9\ P_{tot}$). (b, right) Yield diagram of by-product gas species of Fig. 3a.

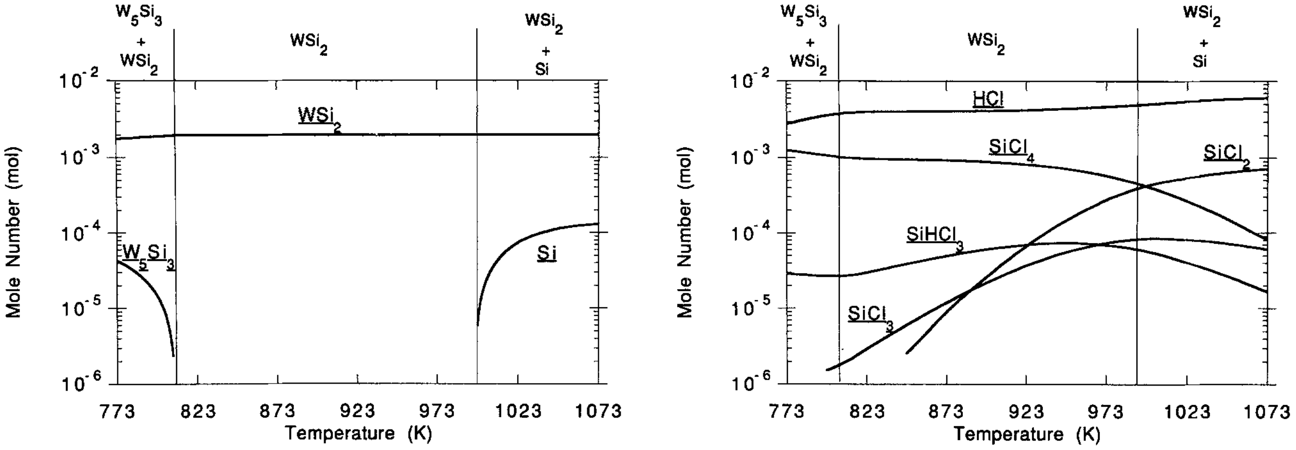

Fig. 4. (a, left) Yield diagram of computed solid phases as a function of deposition temperature for the operating conditions of point B. (b, right) Yield diagram of by-product gas species of Fig. 4a.

parameters. The yield diagrams show the variation in the quantities of different solid phases and by-product gas species as a function of one process parameter (*Rx* or *Td*).

Figure 1 presents a typical CVD phase diagram for 1 Torr total pressure and 873 K deposition temperature for mole fractions of WCl_4 and SiH_4 in the initial gas phase varying from 10^{-5} to 10^{-2}. The reactive gases are diluted in Ar at a pressure of 90% of P_{tot} and the remainder was made up with H_2. The diagram (Fig. 1) can be divided into six possible solid-phase regions: three single-phase domains, WSi_2, W_5Si_3, and W, and three mixed-phase domains, WSi_2 + Si, W_5Si_3 + WSi_2 and W + W_5Si_3, in agreement with the W-Si equilibrium phase diagram. Note that the single-phase domains are separated by mixed-phase domains.

A magnified portion of the top right part of Fig. 1 is given in Fig. 2 in linear coordinates. Points A to E correspond to different experimental conditions investigated as a function of *Rx*. The variations in the quantities of the different solid phases simulated, for the conditions of points A to E of Fig. 2, are presented in the yield diagram of Fig. 3a (the yield diagram of by-product gas species for the same conditions is presented, for reference purposes, in Fig. 3b).

Figures 4a and b show the calculated yield diagrams of solid phases and by-product gas species, respectively, as a function of deposition temperature between 773 and 1073 K. These diagrams were drawn for the operating conditions of point B: $P_{SiH_4} = 5 \times 10^{-3}$ Torr, $P_{WCl_4} = 2 \times 10^{-3}$ Torr, $P_{H_2} = 9.3 \times 10^{-2}$ Torr, $P_{Ar} = 0.9 \times P_{tot}$, $P_{tot} = 1$ Torr and are shown in Fig. 4a and b, respectively.

Using CVD processes, a good blanket and often selective deposition can be obtained by the careful choice of chemical and process parameters such as the nature and the composition of reactant gases, deposition temperature (T_d), and reactor pressure (P_{tot}). With this initial thermodynamic simulation, the conditions required to obtain a pure WSi_2 film were defined and the reactant ratio *Rx* can be varied from 0.4 to 0.5 at constant deposition temperature $T_d = 873$ K or T_d can be modified from 810 to 1210 K at constant *Rx* = 0.4. To check the accuracy of this simulation experimentally, blanket LPCVD WSi_2 films were systematically studied as a function of reactant ratio or deposition temperature (Table I).

Experimental Procedure

The atmospheric pressure CVD reactor used to process $TaSi_2$ and WSi_2 films[21] was converted into an LPCVD reactor. Other transformations were made: modification of the SiH_4 gas line, addition of a lamp heating system, vacuum pump, etc. A quartz tube filled with 99.95% pure tungsten wire (diam = 0.05 mm) and acting as a chlorination chamber, was set up in the LPCVD reactor as shown in Fig. 5. A chlorine line is directly connected to the chlorination chamber and the chamber temperature was controlled with a lamp heating system. The amount of metal chlorides ad-

Table I. Nature and percentage of solid phases predicted by the thermodynamic simulations compared to experimental results.
A. As a function of initial gas phase composition (T_d = 873 K, P_{tot} = 1 Torr, P_{Ar} = 0.9 P_{tot}).

Position in CVD phase diagram	Reactant ratio (*Rx*)	Computed phases	Percentage of solid phases	Experimentally identified phases (XRD)
A	0.3	Si + WSi_2	78:22	Si + h-WSi_2
B	0.4	WSi_2	100	h-WSi_2
C	0.5	WSi_2 + W_5Si_3	97:3	h-WSi_2 + W_5Si_3
D	0.6	WSi_2 + W_5Si_3	80:20	h-WSi_2 + W_5Si_3
E	1.0	W_5Si_3	100	W_5Si_3 + W(Si)

B. As a function of deposition temperature (P_{tot} = 1 Torr, P_{Ar} = 0.9 Torr, P_{H_2} = 0.09 Torr, *Rx* = 0.4).

T_d (K)	Computed phases	Percentage of solid phases	Experimentally identified phases (XRD)
773	WSi_2 + W_5Si_3	97:3	W(Si)
823	WSi_2	100	h-WSi_2 + W_5Si_3
873	WSi_2	100	h-WSi_2
973	WSi_2	100	h-WSi_2 + t-WSi_2 + W_5Si_3
1023	WSi_2 + Si	96:4	h-WSi_2 + t-WSi_2 + W_5Si_3
1073	WSi_2 + Si	95:5	h-WSi_2 + t-WSi_2 + W_5Si_3

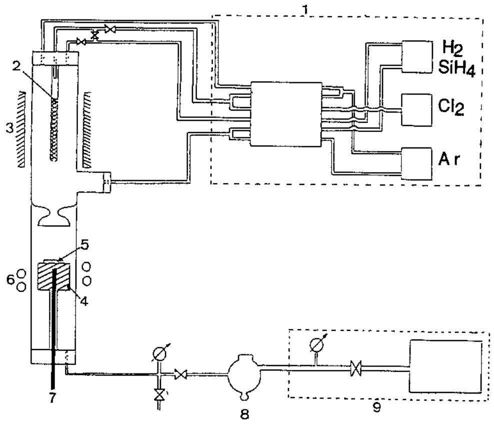

1) **Gases distribution.**
2) **Tungsten wire.**
3) **Lamp furnace.**
4) **Graphite susceptor.**
5) **Wafer.**
6) **RF Coil.**
7) **Thermocouple.**
8) **Cold trap.**
9) **Vacuum system.**

Fig. 5. Schematic diagram of LPCVD reactor.

mitted to the deposition zone is controlled by the amount of chlorine gas released into the chlorination chamber and the chamber temperature, assuming 100% conversion. In the present study, throughout the experiments, the chlorination temperature was kept constant at 1073 K. High purity N55 1% silane in Ar, H_2, Cl_2, and Ar gases were used and their flows were controlled with mass flow controllers. The metal chlorides and other gases generated are mixed in the top section of the deposition zone, and directed to the substrate. An Alcatel chemical pump (Model No. 2063) is used as a vacuum pump and pressure in the reactor is controlled by an MKS-Type 252 exhaust valve controller, Baratron capacitance manometer, PDR-C-1C power supply and digital read-out box which were interfaced with one another. A cold trap is placed between the CVD reactor and the vacuum system to trap solid residues and reactive gases. N-type (111) 10-20 Ω-cm silicon wafers and/or patterned oxidized silicon wafers were used as substrates. After dipping in diluted HF, the cleaned substrates were loaded horizontally on a graphite block and heated with an RF induction heater from 300 to 1200°C.

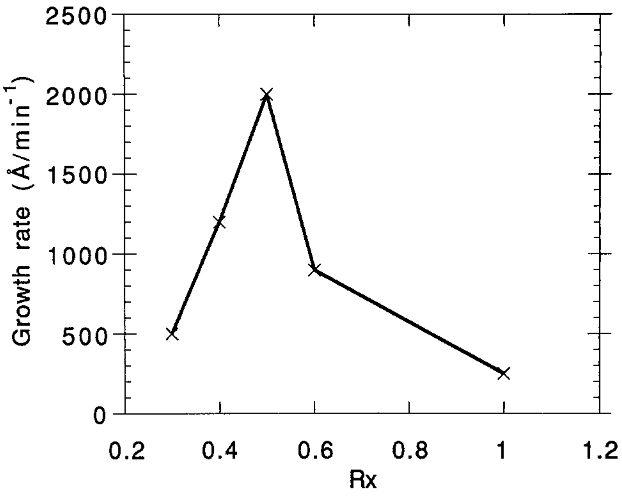

Fig. 6. Growth rate of films as a function of WCl_4/SiH_4 gas ratio.

A typical deposition process is as follows:

1. Prior to deposition, the chlorination chamber was regenerated by heating to 1073 K at a total pressure of 1 Torr under 300 sccm of H_2 for a period of 30 min. This removes any metal oxides or oxychlorides present in the pure W metal chamber.

2. The chamber was cooled to room temperature and the cleaned substrates were loaded, followed by purging of the entire system.

Table II. Summary of process parameters and experimental results of WSi_2 films deposited as a function of reactant ratio ($Rx = WCl_4/SiH_4$). Experimental conditions: deposition temperature: 873 K; deposition time: 10 min; flow of gases (sccm): SiH_4 = 5, Ar = 890; total flow of gases (SiH_4 + Ar + H_2 + WCl_4): 1000 sccm; pressure in the reactor: 133 Pa (1 Torr).

Reactant ratio (*Rx*)	Nature of film	Film thickness (nm)	Film resistivity (μΩ · cm)	Surface morphology	Solid phases identified by XRD in films
0.3	As-deposited	500	10,000	Good surface and smooth interface	h-WSi_2 Si
0.3	Annealed	500	3,250	No significant change	t-WSi_2
0.4	As-deposited	1,200	1,450	Smooth surface and interface	h-WSi_2
0.4	Annealed	1,200	290	No significant change	t-WSi_2 W_5Si_3
0.5	As-deposited	2,000	5,500	Microcracks on surface; smooth interface with columnar growth	t-WSi_2 W_5Si_3
0.5	Annealed	2,000	310	No significant change	W_5Si_3 t-WSi_2
0.6	As-deposited	900	1,000	Rough surface and interface	h-WSi_2 W_5Si_3
0.6	Annealed	900	360	No significant change	t-WSi_2
1.0	As-deposited	250	—	Porous surface and textured interface	W(Si) W_5Si_3

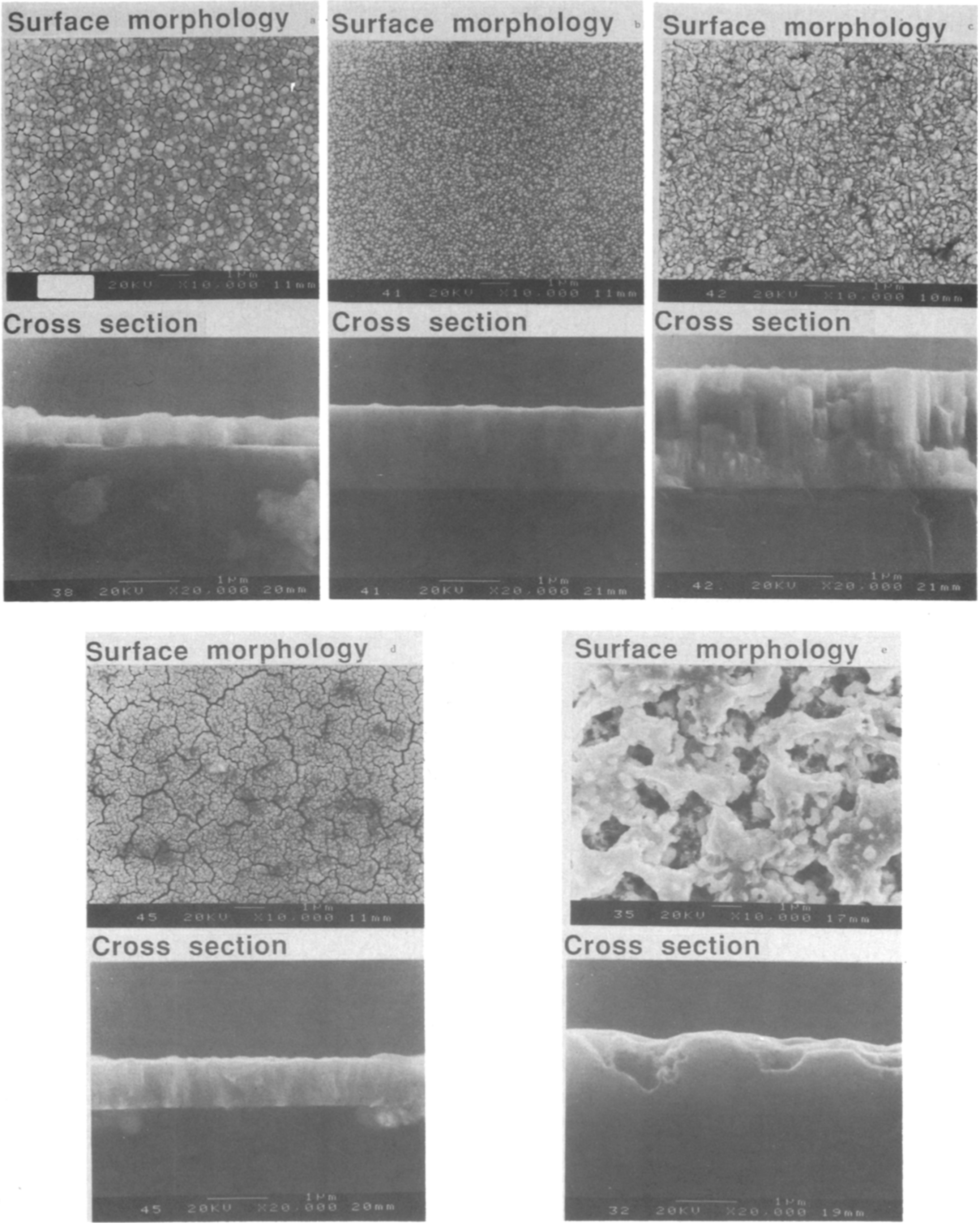

Fig. 7. SEM micrographs of surface morphology and interface texture of films processed at varying reactant ratio: (a) $Rx = 0.3$, (b) 0.4, (c) 0.5, (d) 0.6, and (e) 1.0.

3. Thin polysilicon films were deposited at low pressure on the substrates at 923 K using 1% SiH_4 in Ar to act as a buffer layer to the metal silicide film. The deposition temperature of the substrate and chlorination chamber temperature were then set.

4. When the desired temperatures were obtained, the reactive gases and carrier gases were introduced, depending on process conditions, and shut down after a given deposition time (10 min). Precautions were taken to cool the samples slowly under H_2/Ar atmosphere.

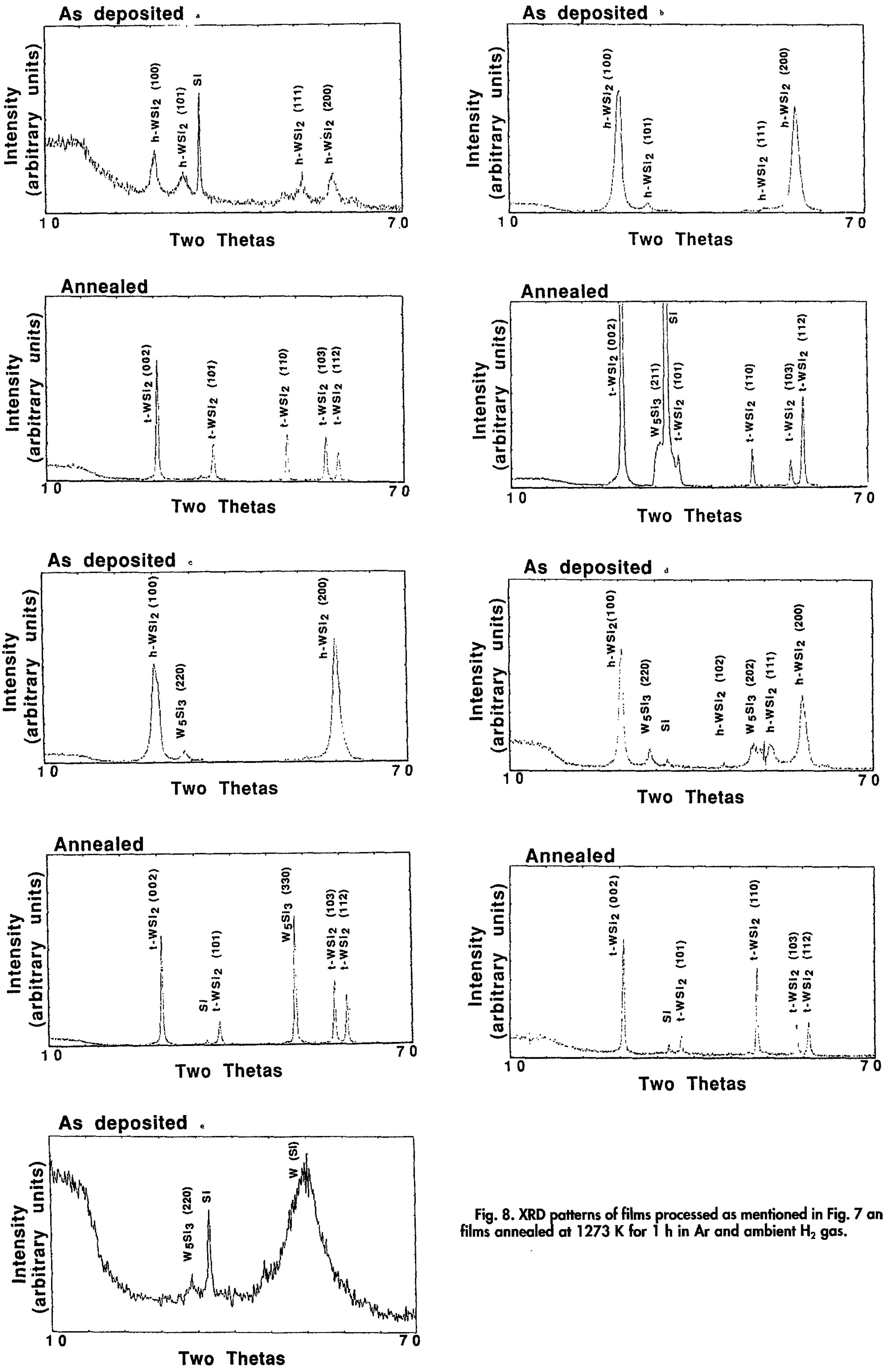

Fig. 8. XRD patterns of films processed as mentioned in Fig. 7 and films annealed at 1273 K for 1 h in Ar and ambient H_2 gas.

5. Some of these films were annealed at 1273 K under 500 sccm of H_2 at a total pressure of 1 Torr for a period of 1 h.

In the present study, two sets of samples were prepared: (*i*) films processed with Rx varying between 0.3 and 1.0 at a constant temperature of 873 K, and (*ii*) films processed with deposition temperature varying from 723 to 1073 K with a constant $Rx = 0.4$ gas mixture. Throughout the experiments the total gas flow of all gases was 1000 sccm and the total pressure was 1 Torr.

The films grown were characterized by studying their phase composition and structural properties by XRD, thickness, surface morphology, and interface texture by SEM, film composition and impurities by AES, and sheet resistance by four-point probe. From XRD patterns, the grain size was calculated using Sherrer's formula.[29,30] To check process reproducibility, the experiments were repeated several times. Little variation was observed in the growth rate of films processed by the same conditions and the results presented here show the typical characteristics of these films.

Results and Discussion

Films processed with variable reactant ratio (Rx): WCl_4/SiH_4.—Table II gives a summary of the process parameters and experimental results of films deposited with reactant ratio varying between 0.3 and 1.0. Figure 6 presents the film growth rate *vs.* Rx at a constant deposition temperature 873 K. It can be seen from this figure that, with increasing reactant ratio from 0.3 to 0.5, the film growth rate increases from 500 to 2000 Å/min, while any further increase in reactant ratio above 0.5 decreases the growth rate. SEM studies revealed that films grown at $Rx < 0.5$ are characterized by a smooth surface and interface as shown in Fig. 7a, b, and c. However, as Rx increases above 0.5, this leads to the formation of surface microcracks, Fig. 7d and a porous surface and textured interface Fig. 7e. Annealing the as-grown films did not affect the surface morphology.

XRD studies show that film composition is strongly dependent on reactant ratio and/or annealing conditions. Figure 8 shows XRD patterns of silicide films deposited on silicon substrates. For the three points (A, B, and C), some experiments have shown that the XRD patterns of the silicide films deposited on SiO_2 substrates are similar to those obtained with Si substrates. Figure 8a shows XRD patterns of films obtained for $Rx = 0.3$ as-deposited and annealed. The as-deposited films show polycrystalline hexagonal WSi_2 phase (noted h-WSi_2), which correspond to the low temperature structure, with strong (100), (200) reflections. The typical grain size of h-WSi_2 with (h00) orientation, calculated by Sherrer's formula, is about 90-100 Å. By annealing, the films obtained on SiO_2 are converted into pure tetragonal WSi_2-phase (high temperature structure) (noted t-WSi_2) with strong (002), (110), and (103) reflections. The sharp peaks of annealed films are indicative of better crystallinity and the typical grain size of t-WSi_2 is about 400 Å. Films obtained with $Rx = 0.4$ give pure h-WSi_2 with strong (100) and (200) peaks as shown in Fig. 8b. By annealing, the films deposited on SiO_2 give the t-WSi_2 phase with, in addition, a small peak of W_5Si_3. Increasing Rx to 0.5 results in the appearance of W_5Si_3 phase in addition to strong h-WSi_2 peaks. On annealing the films obtained on SiO_2, the W_5Si_3 peak is enhanced and the h-WSi_2 phase is converted into t-WSi_2 as shown in Fig. 8c. When Rx is increased even further ($Rx > 0.6$), the films grow almost selectively on Si and have metal-rich phases. The XRD patterns of as-deposited films at $Rx = 0.6$ show an increase in W_5Si_3 peaks and a further increase in Rx to 1.0 results in pure metal-rich phases, W_5Si_3 and W(Si) (W with silicon traces), as shown in Fig. 8d and 8e, respectively. Figure 8e shows that the metal-rich phases have fine grains, as indicated by their broad XRD peaks. By annealing, the films deposited on Si are converted into t-WSi_2 phase (Fig. 8d) for all these experimental conditions.

Collating the data obtained, it appears that the growth rate of films with varying reactant ratio reaches a maximum at $Rx = 0.5$. Increasing growth rate with reactant ratio indicates that the film growth rate is controlled by the WCl_4 input rate. A further increase in Rx decreases the film growth rate and enhances the formation of metal-rich phases. It has been reported that Si-rich WSi_2 films have a good surface morphology and smooth film/substrate interface.[8] In the present study, the films processed with $Rx < 0.5$ also have a smooth surface and interface. However, the porous surface and textured interface of films deposited at $Rx = 1.0$ may be attributed to attack of the Si substrate by chloride species. XRD patterns of as-deposited films with varying Rx show different solid phases in good agreement with thermodynamic simulations. The strong reflections of (h00) h-WSi_2 in as-grown films indicate that the films grow preferentially in this direction. It is known that, on annealing, the as-deposited WSi_2 films will convert into t-WSi_2 phase. Low temperature WSi_2 films deposited on Si convert into t-WSi_2 easily compared to those on SiO_2 layers. It has also been reported that films with a ratio x = Si:W on SiO_2 substrates will convert completely into t-WSi_2, if $x > 2.3$ whereas, if $x < 2.3$, both W(Si) and t-WSi_2 phases can be detected.[31] In the present study the annealed films (Fig. 8a, $Rx = 0.3$) show pure t-WSi_2 phase indicating that the as-grown films are silicon rich as predicted by thermodynamic simulations. The presence of small peaks of W_5Si_3 phase in annealed films processed at $Rx = 0.4$ (Fig. 8b) may be attributed to a slight deficiency of Si in the as-grown films.

Table Ia shows that the thermodynamic CVD-phase diagram agrees quite well with the experimentally observed solid phase.

The as-deposited films have a resistivity of a few thousand Ω-cm (Table II), which is quite high but not unusual for films deposited at low temperature. On annealing the

Table III. Influence of deposition temperature (T_d) on film properties. Experimental conditions: deposition time = 10 min. Gas flow (sccm): $SiH_4 = 5$, $WCl_4 = 2$, $H_2 = 100$, $Ar = 893$ (total = 1000).

T_d (K)	Film thickness (nm)	Film resistivity (μΩ · cm)	Surface morphology
773	150	—	Porous surface and textured interface
823	300	1140	Microcracks on the surface
873	1200	1450	Smooth surface and interface
973	1500	5610	Small platelets on surface; smooth interface having columnar growth
1023	1650	5440	Small platelets on surface; smooth interface having columnar growth
1073	2000	2200	Increase in platelet size

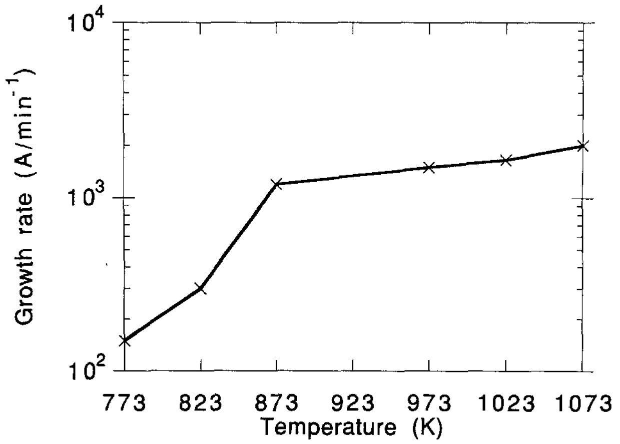

Fig. 9. Growth rate of films processed at a constant reactant ratio $Rx = 0.4$.

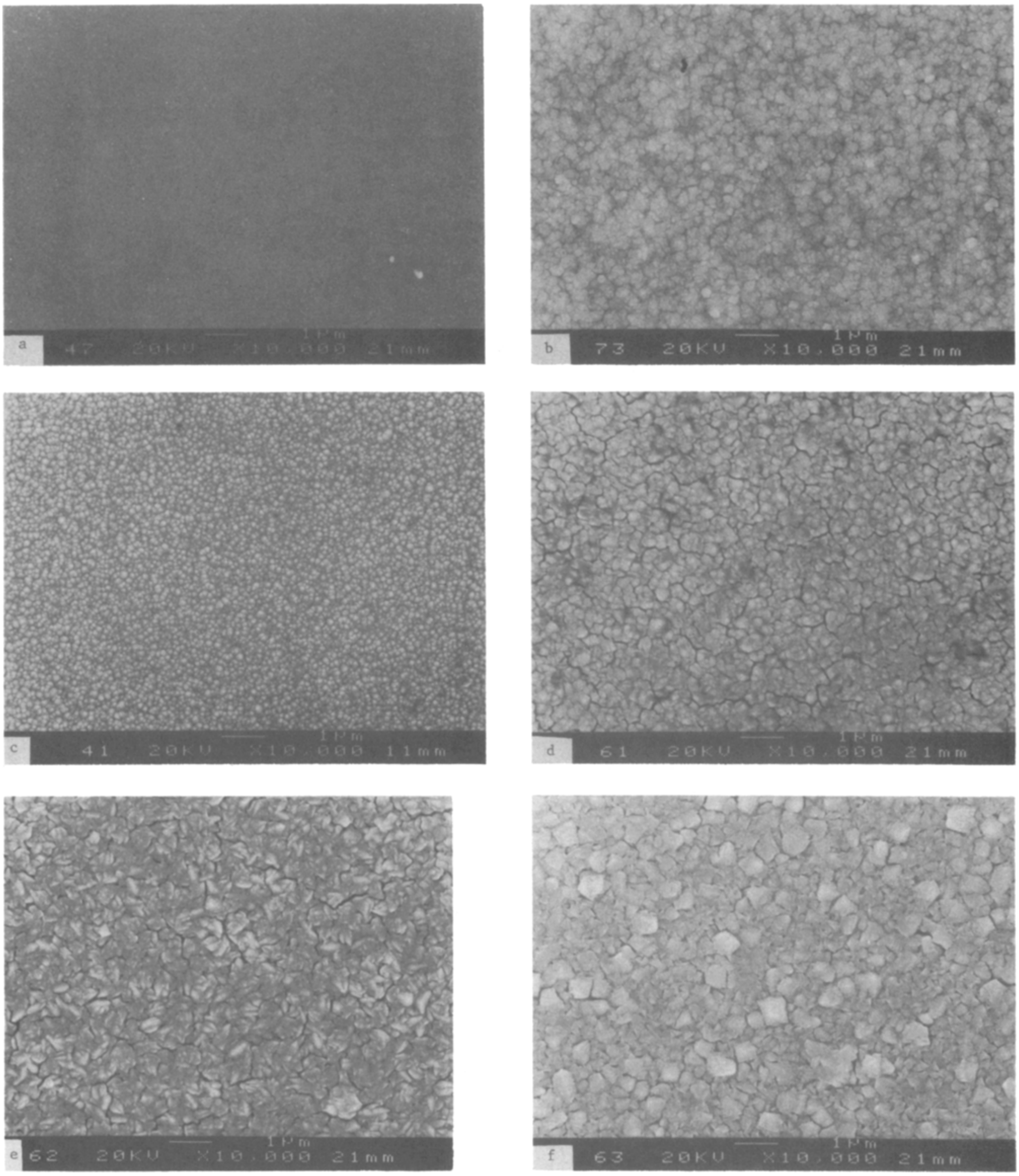

Fig. 10. SEM micrographs of surface morphology of films processed at various temperatures: (a) 773, (b) 823, (c) 873, (d) 973, (e) 1023, and (f) 1073K.

films, the resistivity decreases to a few hundred μΩ-cm. However, the films processed at high SiH_4 partial pressure ($Rx = 0.3$) have high resistivity values even after annealing.

Effect of deposition temperature.—To study the effect of deposition temperature on the metal silicide deposits using the chloride chemistry, thin films were processed with varying deposition temperature from 773 to 1073 K, at a constant reactant ratio $Rx = 0.4$. Table III presents a summary of the process parameters and experimental results obtained for such films. The growth rate of films as a function of the deposition temperature shows two regions: linear increase of growth rate at low temperatures (<923 K) and saturation at higher temperatures as shown in Fig. 9. SEM micrographs reveal that films processed at 773 K have a porous surface and rough interface. Films deposited between 823 and 923 K have a smooth surface and interface. Platelet growth was observed on the surface of films processed above 823 K, and the size of the platelets increases with temperature as shown in Fig. 10a-f. XRD patterns of films deposited at various temperatures are shown in Fig. 11a-f. It can be seen from the XRD peaks that the films processed have, respectively, sharp peaks of W(Si) at 773 K, high intensity peaks of W_5Si_3 phases plus h-WSi_2 at 823 K, pure h-WSi_2 phase at 873 K, and various mixed phases above 923 K. The resistivity of as-deposited films is of the order of a few thousand Ω-cm and decreases with increasing deposition temperature.

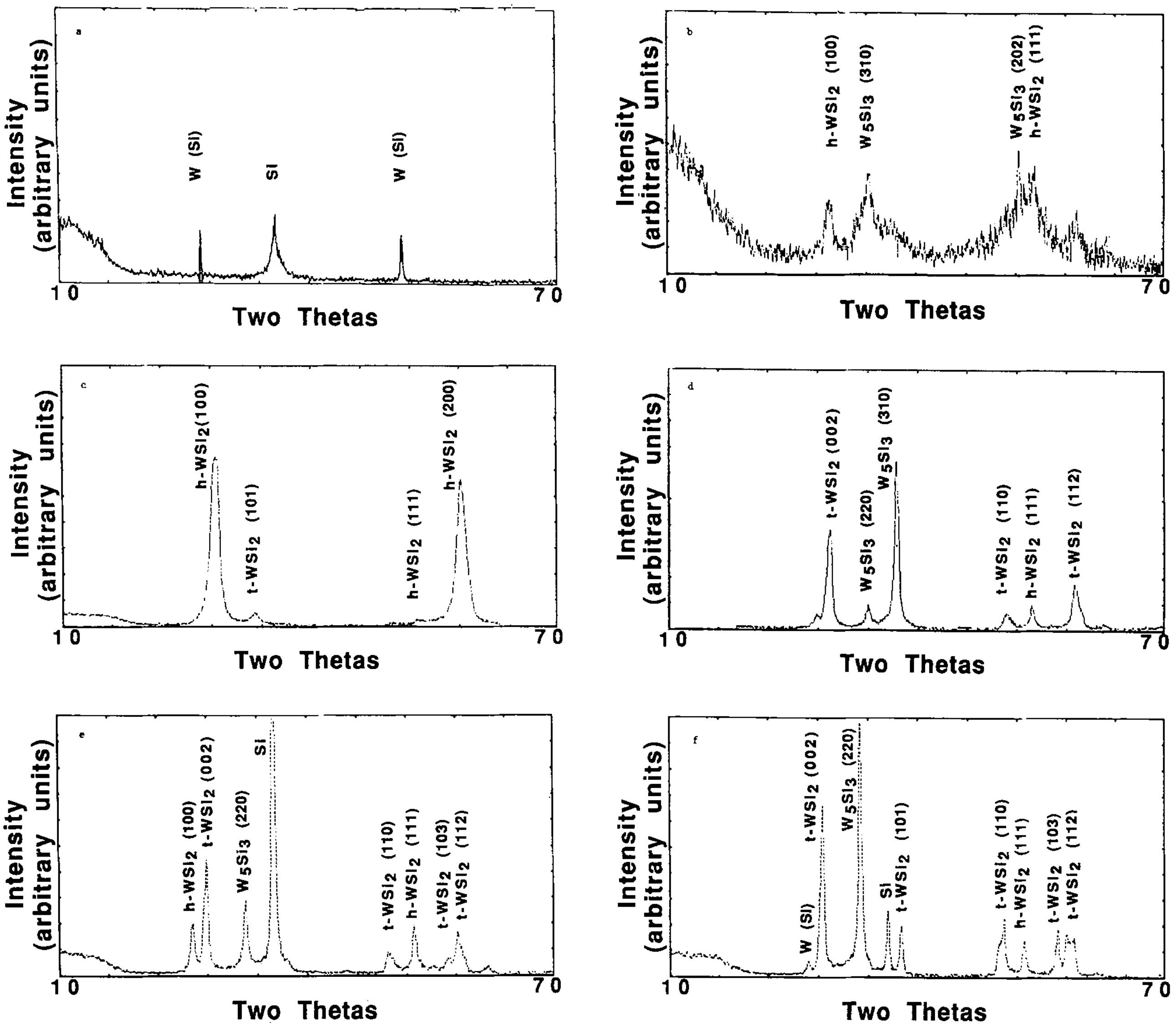

Fig. 11. XRD patterns of films processed as mentioned in Fig. 10.

The comparison between thermodynamically expected and experimentally observed phases, as given in Table Ib, shows that the as-deposited mixed phases above 923 K are in disagreement with the calculations, perhaps because the phase-transition hexagonal/tetragonal is not very well included in WSi_2 thermodynamic description. At low temperature, the films are composed by W-rich phases, as predicted by thermodynamic calculations.

Selectivity.— On the basis of the above-mentioned studies of reactant ratio and deposition temperature, a set of process parameters has been defined ($Rx = 0.4$, $T_d = 873$ K, $P_{total} = 1$ Torr) for the selective growth of WSi_2 films on fine-patterned oxidized Si. The native oxide on Si was etched with a small flow (0.5 sccm) of silane in Ar for 3 to 10 min, at 873 K, prior to film deposition. Etching of the native oxide with SiH_4 was found to be more effective than classical etching with H_2. The small amount of silicon resulting from the decomposition of SiH_4 reacts with SiO_2 and forms SiO gas prior to deposition of Si. Hence, the optimization of silane flow and etching time plays a very important role in achieving good selectivity. In the present study selective WSi_2 films were processed by varying etching time of the native oxide and/or deposition time, at $T_d = 873$ K and $Rx = 0.4$. SEM micrographs of selective WSi_2 films deposited for 10 min (native oxide etching time: 4 min) are shown in Fig. 12. The micrographs show that the films were selectively grown on Si, and that the surface morphology is very smooth. Figure 13 presents the Auger spectrum of selective LPCVD WSi_2 films, which show little film contamination by impurities such as carbon, chlorine, and oxygen.

Conclusions

An experimental study of tungsten disilicide low pressure CVD, with variable reactant ratio and deposition tem-

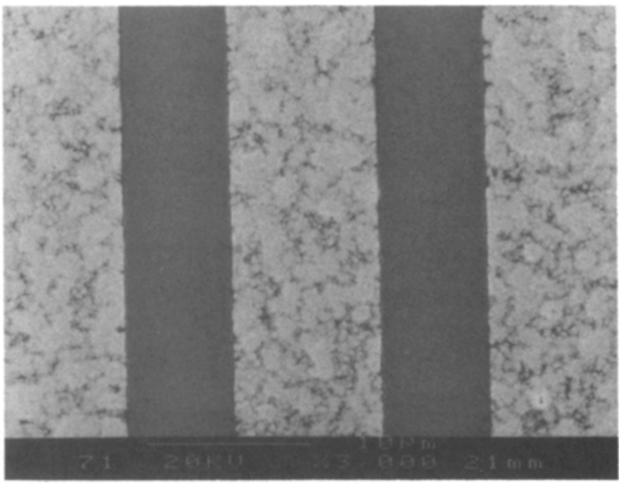

Fig. 12. SEM micrographs of selective LPCVD WSi_2 films processed on fine-patterned oxidized silicon substrates.

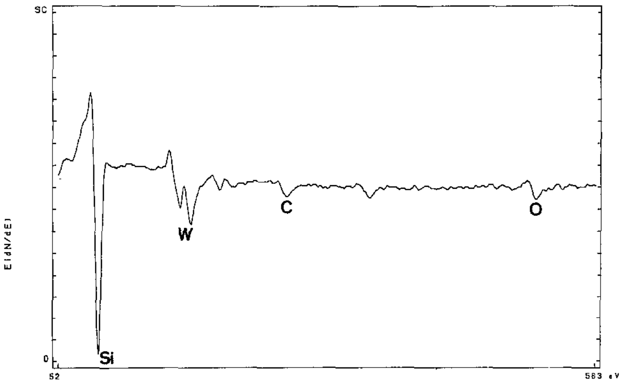

Fig. 13. Auger spectrum of LPCVD WSi_2 films processed at T_d = 873 K and Rx = 0.4.

perature, was carried out, which was preceded by an initial thermodynamic simulation of the process.

Submicronic blanket WSi_2 films were deposited at T_d = 873 K and P_{tot} = 133 Torr from a gaseous phase composed of SiH_4, WCl_4 (Rx = 0.4), H_2, and Ar. Their morphology and resistivity are compatible with the latest microelectronic technology requirements.

The agreement between the thermodynamic simulation and the experimental results is quite good.

It was possible to process selective LPCVD WSi_2 films on fine-patterned oxidized silicon wafers. The films grown show good selectivity and a smooth surface indicating that chloride-based chemistry could be used for the synthesis of selective WSi_2 films for VLSI technology.

Acknowledgments

The authors would like to thank the French National Telecommunications Centre (CNET) for financial and technical support. One of the authors (P.S.N.) is grateful to the CEC for awarding a PDF, and to the Director of CEERI Pilani for his constant encouragement during this work.

Manuscript submitted June 22, 1992; revised manuscript received Sept. 2, 1992.

LTPCM—ENSEEG assisted in meeting the publication costs of this article.

REFERENCES

1. S. Wolf and R. N. Tauber, *Silicon Processing for the VLSI Era,* Vol. 1: *Processing Technology,* p. 384, Lattice Press, Sunset Beach, CA (1988).
2. T. Hara, S. Enomoto, and T. Jinbo, *Jpn. J. Appl. Phys. Lett.,* **23,** L455 (1984).
3. L. D. Locker and C. D. Capio, *J. Appl. Phys.,* **44,** 4366 (1973).
4. B. L. Crowder and S. Zirinsky, *IEEE Trans. Electron Devices,* **ED-26,** 369 (1979).
5. T. P. Chow, D. H. Bower, R. L. Van Art, and W. Katz, *This Journal,* **130,** 952 (1983).
6. Y. Shioya and M. Maeda, *J. Appl. Phys.,* **60,** 327 (1986).
7. D. L. Brors, J. A. Fair, K. A. Monning, and K. C. Saraswat, *Solid State Technol.,* 183 (1983).
8. K. C. Saraswat, D. L. Brors, J. A. Fair, K. A. Monnong, and R. Beyers, *IEEE Trans. Electron Devices,* **ED-30,** 1497 (1983).
9. C. M. Osburn, M. Y. Tsai, S. Roberts, C. J. Lucchese, and C. Y. Ting, in *VLSI Science and Technology/1982,* C. J. DelPoca and W. M. Bullis, Editors, PV 82-7, p. 213, The Electrochemical Society Softbound Proceedings Series, Pennington, NJ (1982).
10. T. P. H. F. Wendling, C. Wieczorek, and K. Hieber, in *Proceedings of 2nd European Workshop on Refractory Metals and Silicides,* p. 255, Aussois, France (1987).
11. R. Madar, E. Mastromatteo, C. Vahlas, C. Bernard, J. Palleau, and J. Torres, in *Proceedings of the MRS Fall Meeting,* Boston, MA (1988).
12. E. Mastromatteo, Ph.D. Thesis, LMPG-INP, Grenoble, France (1991).
13. K. Shenai, P. A. Piacente, R. Saia, and B. J. Baliga, *IEEE Trans. Electron Devices,* **10,** 270 (1989).
14. M. L. Hitchman, A. D. Jobson, and L. F. T. Kwakwan, *Appl. Surf. Sci.,* **38,** 312 (1989).
15. M. L. Green and R. A. Levy, *This Journal,* **132,** 444 (1985).
16. H. H. Busta and C. H. Tang, *ibid.,* **133,** 1195 (1986).
17. C. Bernard, C. Vahlas, J. F. Million-Brodaz, and R. Madar, in *Tenth International Conference on Chemical Vapor Deposition/1987,* G. W. Collen, Editor, PV 87-8, p. 700, The Electrochemical Society Softbound Proceedings, Pennington, NJ (1987).
18. C. Vahlas, G. Baret, J. F. Million-Brodaz, C. Bernard, and R. Madar, in *Proceedings of 6th European Conference on CVD,* R. Porat, Editor, p. 255, Jerusalem (1987).
19. S. L. Zhang, R. Buchta, Y. F. Wang, E. Niemi, J. T. Wange, and C. S. Petersson, in *Tenth International Conference on Chemical Vapor Deposition/1987,* G. W. Cullen, Editor, PV 87-8, p. 135, The Electrochemical Society Softbound Proceedings Series, Pennington, NJ (1987).
20. A. Harsta and J. O. Carlsson, *Thin Solid Films,* **176,** 263 (1989).
21. E. Blanquet, C. Vahlas, R. Madar, J. Palleau, J. Torres, and C. Bernard, *Thin Solid Films,* **177,** 189 (1989).
22. E. Blanquet, N. Thomas, C. Vahlas, J. C. Obelin, J. Torres, R. Madar, and C. Bernard, in *Eleventh International Conference on Chemical Vapor Deposition/1990,* K. E. Spear and G. W. Cullen, Editors, PV 90-12, p. 474, The Electrochemical Society Softbound Proceedings Series, Pennington, NJ (1990).
23. N. Thomas, E. Blanquet, C. Vahlas, C. Bernard, and R. Madar, in *Proceedings of the MRS Fall Meeting,* p. 451, Boston, MA (1990).
24. C. Bernard, *High Temp. Sci.,* **27,** 131 (1990).
25. C. Bernard, Y. Deniel, A. Jacquot, P. Vay, and M. Ducarroir, *J. Less Common Metals,* **40,** 165 (1975).
26. C. Vahlas, P. Y. Chevalier, and E. Blanquet, in *Proceedings of the 13th Calphad Meeting,* No. 3, p. 273 (1989).
27. J. N. Barbier and C. Bernard, in *Proceedings of the 15th Calphad Meeting,* L. Kaufman, Editor, p. 206 (1986).
28. M. Ducarroir, M. Jaymes, C. Bernard, and Y. Deniel, *J. Less Common Met.,* **40,** 173 (1975).
29. P. Scherrer, *Gottinger Nachrichten,* **2,** 98 (1918).
30. H. P. Klug and L. E. Alexander, *X-ray Diffraction Procedures for Polycrystalline and Amorphous Materials,* p. 491, John Wiley & Sons, Inc., New York (1966).
31. J. R. Chen, Y. K. Fang, and S. L. Hsu, *Vacuum,* **37,** 357 (1985).